Micromechanical Circuits for Wireless Communications

Clark T.-C. Nguyen

Center for Integrated Microsystems
Department of Electrical Engineering and Computer Science
University of Michigan
Ann Arbor, Michigan 48109-2122
email: ctnguyen@eecs.umich.edu

Abstract

Micromechanical communication circuits fabricated via IC-compatible MEMS technologies and capable of low-loss filtering, mixing, switching, and frequency generation, are described with the intent to miniaturize wireless transceivers. A possible transceiver front-end architecture is then presented that uses these micromechanical circuits in large quantities to substantially reduce power consumption. Technologies that integrate MEMS and transistor circuits into single-chip systems are then reviewed with an eye towards the possibility of single-chip communication transceivers.

1. Introduction

Due to their need for high frequency selectivity and low noise frequency manipulation, portable wireless communication transceivers continue to rely on off-chip resonator technologies that interface with transistor electronics at the board-level. In particular, highly selective, low loss radio frequency (RF) and intermediate frequency (IF) bandpass filters generally require ceramic, SAW, or quartz acoustic resonator technologies with Q's in excess of 1,000. In addition, LC resonator tanks with Q's greater than 40 are required by voltage-controlled oscillators (VCO's) to achieve sufficiently low phase noise. These off-chip resonator components then contribute to the substantial percentage (often up to 80%) of portable transceiver area taken up by board-level, passive components.

Recent advances in IC-compatible micro-electromechanical system (MEMS) technologies that make possible micro-scale, mechanical circuits capable of low-loss filtering, mixing, switching, and frequency generation, now suggest methods for boardless integration of wireless transceiver components. In fact, given the existence already of technologies that merge micromechanics with transistor circuits onto single silicon chips [1]-[7], single-chip transceivers may eventually be possible, perhaps using alternative architectures that maximize the use of passive, high-Q, micromechanical circuits to reduce power consumption for portable applications.

This paper presents an overview of the micromechanical circuits and associated technologies expected to play key roles in reducing the size and power consumption of future communication transceivers.

2. Micromechanical Circuits

Although mechanical circuits, such as quartz crystal resonators and SAW filters, provide essential functions in the majority of transceiver designs, their numbers are generally suppressed due to their large size and finite
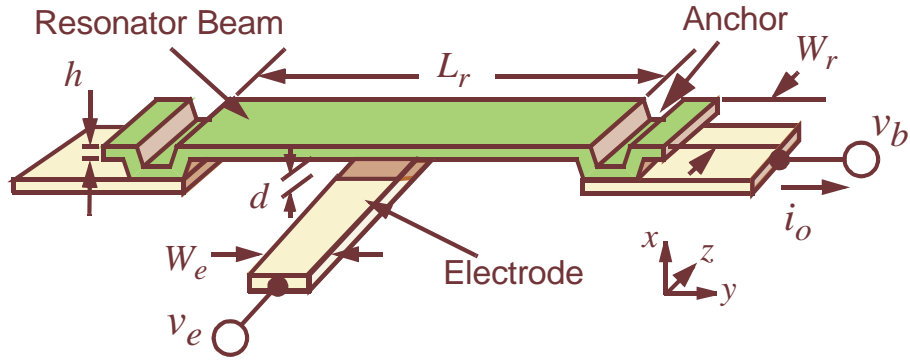
Figure 1: Perspective-view schematic of a clamped-clamped beam μmechanical resonator in a general bias and excitation configuration.

cost. Unfortunately, when minimizing the use of high-Q components, designers often trade power for selectivity (i.e., Q), and hence, sacrifice transceiver performance.

By shrinking dimensions and introducing batch fabrication techniques, MEMS technology provides a means for relaxing the present constraints on the complexity of mechanical circuits, with implications not unlike those that integrated circuit technology had on transistor circuit complexity. Before exploring the implications, specific μmechanical circuits are first reviewed.

2.1. Micromechanical Beam Element

To date, the majority of μmechanical circuits most useful for communication applications have been realized using simple μmechanical flexural-mode beam elements, such as shown in Fig. 1 with clamped-clamped boundary conditions. Although several micromachining technologies are available to realize such an element in a variety of different materials, surface micromachining has been the preferred method for μmechanical communication circuits, mainly due to its flexibility in providing a variety of beam end conditions and electrode locations, and its ability to realize very complex geometries with multiple levels of suspension.

Figure 2 summarizes the essential elements of a typical surface-micromachining process

that produces a clamped-clamped beam. In this process, a series of film depositions and lithographic patterning steps—identical to similar steps used in planar IC fabrication technologies—are utilized to first achieve the cross-section shown in Fig. 2(a). Here, a sacrificial oxide layer supports the structural polysilicon material during deposition, patterning, and subsequent annealing. In the final step of the process, the wafer containing cross-sections similar to Fig. 2(a) is dipped into a solution of hydrofluoric acid, which etches away the sacrificial oxide layer without significantly attacking the polysilicon structural material. This leaves the free-standing structure shown in Fig. 2(b), capable of movement in multiple dimensions, if necessary, and more importantly, capable of vibrating with high Q and good temperature stability, with temperature coefficients on the order of -10 ppm/^oC [8].

For frequency reference, filtering, and mixing applications, the resonance frequency of this flexural-mode mechanical beam is of great interest. For the clamped-clamped beam of Fig. 1, the expression for resonance frequency can be written as (ignoring stress and finite width effects) [9]

$$f_o = \frac{1}{2\pi}\sqrt{\frac{k_r}{m_r}} \cong 1.03\kappa\sqrt{\frac{E}{\rho}}\frac{h}{L_r^2}(1-g(V_P))^{1/2}, \quad (1)$$

where E and ρ are the Young's modulus and density of the structural material, respectively;
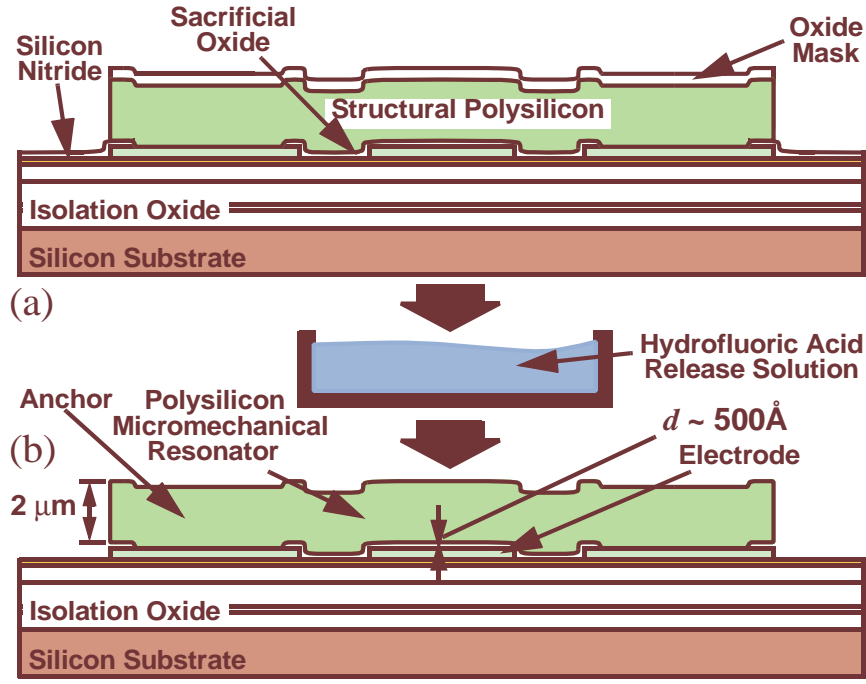
Figure 2: Cross-sections describing surface micromachining. (a) Required film layers up to the release etch step. (b) Resulting free-standing beam following a release etch in hydrofluoric acid.

Table I: μMechanical Resonator Frequency Design*

Freq. [MHz]	Material	Mode	h_r [μm]	W_r [μm]	L_r [μm]
70	silicon	1	2	8	14.54
110	silicon	1	2	8	11.26
250	silicon	1	2	4	6.74
870	silicon	2	2	4	4.38
1800	silicon	3	1	4	3.09
1800	diamond	3	1	4	6.16

* Determined for free-free beams using Timoshenko methods that include the effects of finite h and W_r [13].

h and L_r are specified in Fig. 1; and κ is a scaling factor that models the effects of surface topography in actual implementations [9], [10]. From (1), geometry clearly plays a major role in setting the resonance frequency, and in practice, attaining a specified frequency amounts to CAD layout of the proper dimensions. Table I presents expected resonance frequencies for various beam dimensions, modes,

and structural materials, showing a wide range of attainable frequencies, from VHF to UHF.

To complete the mechanical circuit element, input and output ports are required. These can be either electrical or mechanical, and in any number. In Fig. 1, two electrical inputs are shown, v_e and v_b, applied to the electrode and beam, respectively. In this configuration, the difference voltage (v_e-v_b) is effectively applied across the electrode-to-resonator capacitor gap, generating a force between the stationary electrode and movable beam given by

$$F_d = -\frac{\partial E}{\partial x} = -\frac{1}{2}(v_e - v_b)^2\frac{\partial C}{\partial x}, \qquad (2)$$

where x is displacement (with direction indicated in Fig. 1), and $(\partial C/\partial x)$ is the change in resonator-to-electrode capacitance per unit displacement.

2.2. HF Micromechanical Reference Tank

The high Q and thermal stability of the reso-

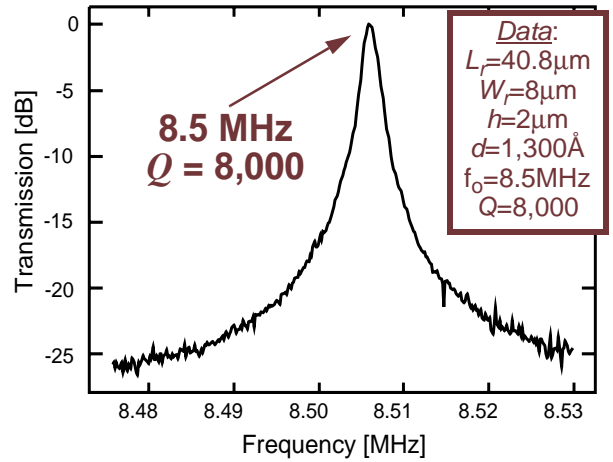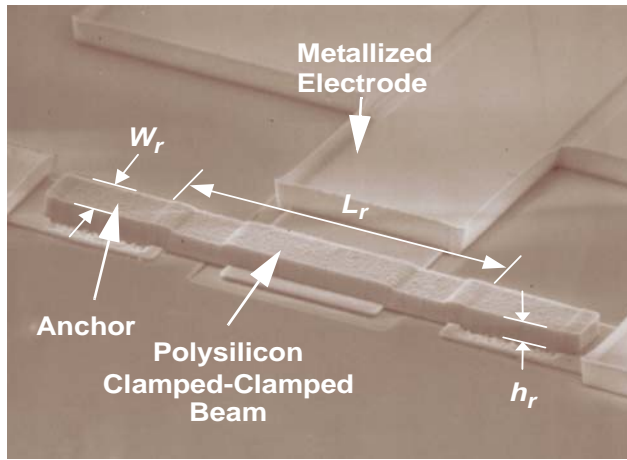Figure 3: SEM of an 8.5 MHz clamped-clamped beam μmechanical resonator with a typical measured spectrum [9].

nance frequency of single μmechanical beam elements make them good candidates for tanks in reference oscillator applications. When using the resonator as a tank or filter circuit (as opposed to a mixer, to be discussed later), a dc-bias voltage V_P is applied to the conductive beam, while an ac excitation signal $v_i=V_i\cos\omega_i t$ is applied to the underlying electrode. In this configuration, a dominant force component is generated at ω_i, which drives the beam into mechanical resonance when $\omega_i=\omega_o$, creating a dc-biased (via V_P) time-varying capacitance between the electrode and resonator, and sourcing an output current $i_o=V_P(\partial C/\partial x)(\partial x/\partial t)$, as shown in Fig. 1. When plotted versus the frequency of v_i, i_o traces out a bandpass biquad characteristic with a $Q\sim10,000$ in vacuum (c.f., Fig. 3)—very suitable for reference oscillators.

2.3. VHF Micromechanical Reference Tank

Although impressive at HF, the clamped-clamped beam device of Fig. 3 begins to lose a substantial fraction of its internal energy to the substrate at frequencies past 30 MHz, and this limits the attainable Q at VHF. One approach to retain high Q as frequencies go beyond 30 MHz is to miniaturize the resonator to the submicron or nano-scale, where its stiffness can be restrained to smaller values so as to reduce energy radiation into the substrate via anchors. Although used successfully to attain mid-VHF frequencies [11], this approach sacrifices the power handling capability (or dynamic range) of the device, possibly rendering it unusable for communications applications where co-site interference is a problem [9], [12]. To retain Q's around 8,000 at VHF while also maintaining a high stiffness for sufficient power handling ability, a beam with free-free ends can be used, such as shown in Fig. 4, in which additional mechanical circuit complexity is added to allow free-free operation, and to reduce anchor losses to the substrate [13]. Via proper support beam design, anchor losses can be greatly attenuated in this structure, and Q's on the order of 8,000 are attained even at 92 MHz.

2.4. Micromechanical Filters

Among the more useful μmechanical circuits for communications are those implementing low-loss bandpass filters. Figure 5(a) presents the SEM of a two-resonator 68 MHz μmechanical filter, comprised of three mechanical links interconnected in a network designed to yield the bandpass spectrum
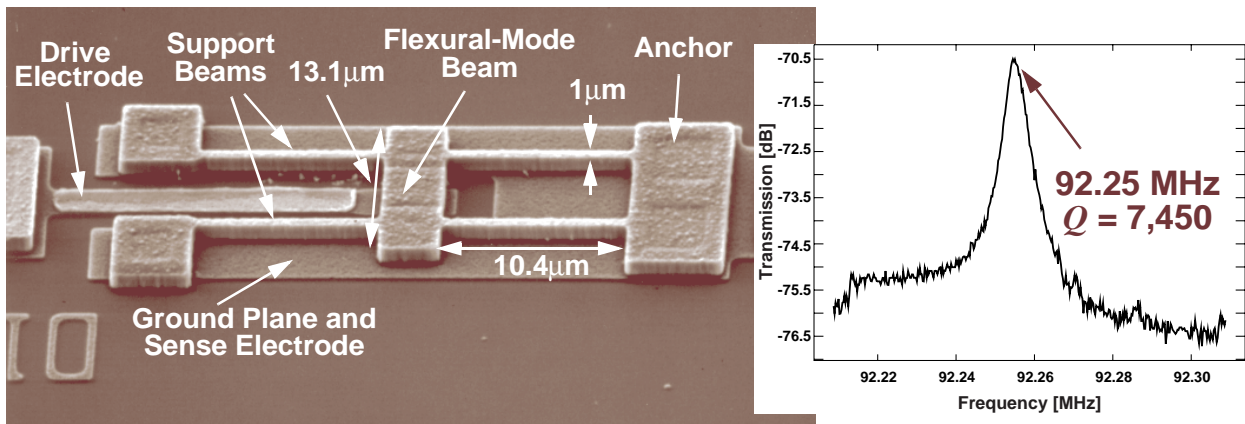
Figure 4: SEM and measured frequency characteristic for a 92 MHz free-free beam polysilicon μmechanical resonator [13].
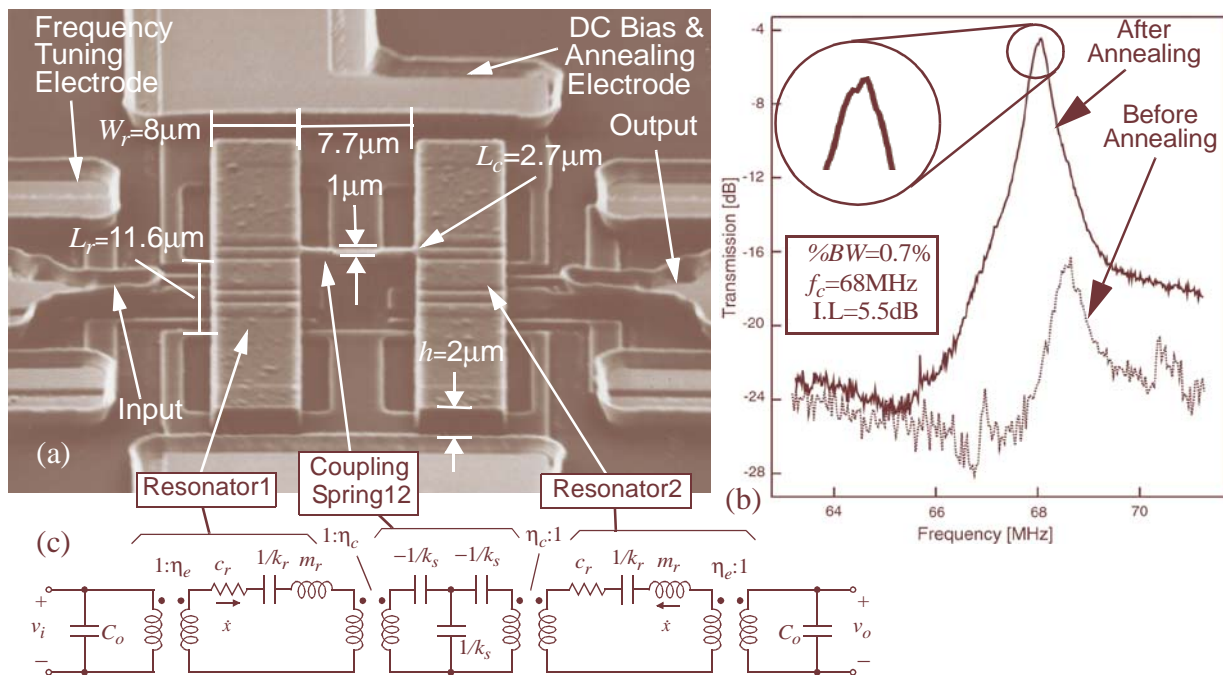

Figure 5: (a) SEM of a 68 MHz two-resonator μmechanical filter. (b) Measured frequency characteristics. (c) Equivalent circuit [14].

shown in Fig. 5(b). The design of this filter has been covered extensively in previous literature [9]. For the present purposes, however, the operation of this filter can be deduced from its equivalent circuit, shown in Fig. 5(c). Here, each of the outside links serve as capacitively transduced μmechanical resonators with equivalent circuits based on *LCR* networks. The connecting link actually operates as an acoustic transmission line, and thus, can be modeled by a *T*-network of energy storage ele-

ments. When combined together into the circuit of Fig. 5(c), these elements provide a more selective filtering function, with sharper roll-offs and increased stopband rejection over single resonator devices.

Note that Fig. 5 depicts a relatively simple mechanical circuit. Using more complicated interconnections with a larger number of beam elements and I/O ports, a wide variety of signal processing transfer functions can be realized, with even wider application ranges.
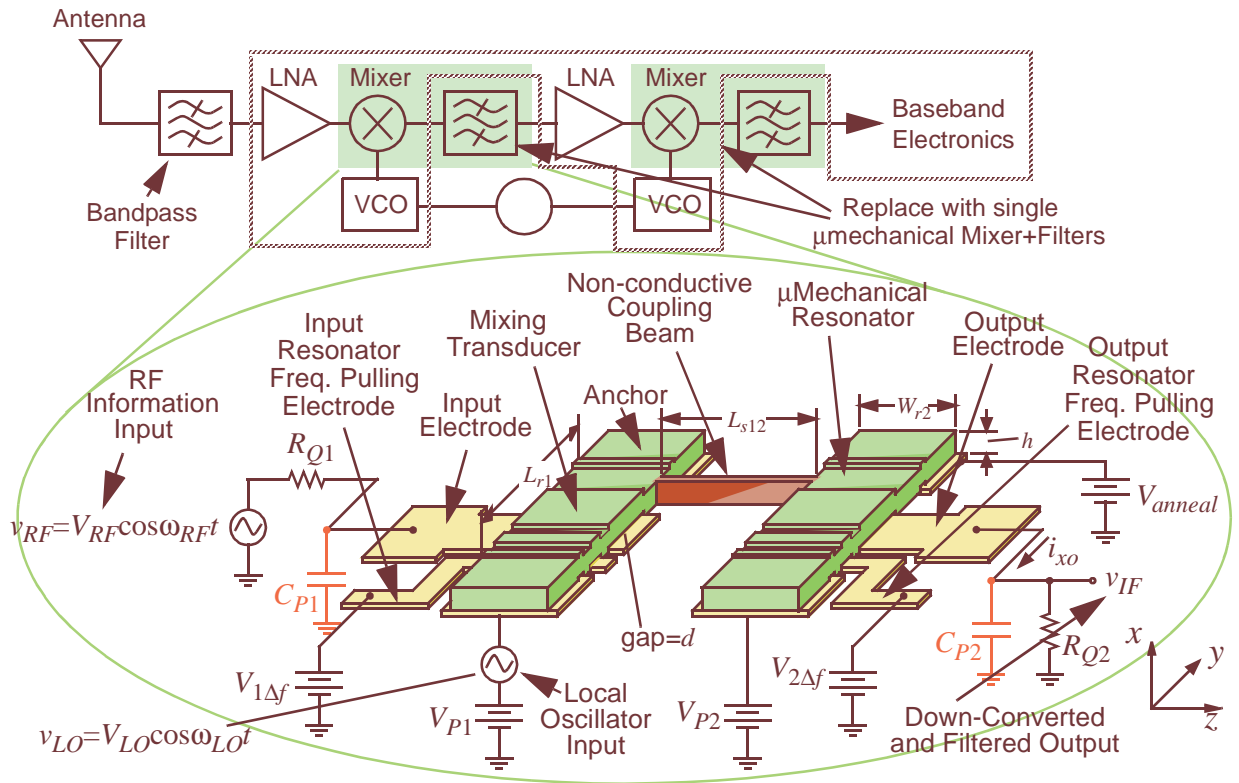
Figure 6: Schematic diagram of a μmechanical mixer-filter, depicting the bias and excitation scheme needed for down-conversion, and showing its use within a receiver [15].

2.5. Micromechanical Mixer-Filters

As indicated by (2), the voltage-to-force transducer of Fig. 1 is nonlinear, relating input force F_d to input voltage $(v_e - v_b)$ by a square law. When $v_b = V_P$ (i.e., a dc voltage), this nonlinearity is suppressed, leading to a dominant force that is linear with v_e. If, however, signal inputs are applied to both v_e and v_b, a square law mixer results, that multiplies v_e and v_b, mixing these two input voltages down to a force component at their difference frequency. In particular, if an RF signal v_{RF} at frequency ω_{RF} is applied to electrode e, and a local oscillator signal v_{LO} at frequency ω_{LO} to electrode b, then these *electrical* signals are mixed down to a *force* signal at frequency $\omega_{IF} = (\omega_{RF} - \omega_{LO})$. If the above transducer is used to couple into a μmechanical filter with a passband centered at ω_{IF} (c.f., Fig. 6), an effective mixer-filter device results that provides both mixing and

filtering in one passive, μmechanical device [15]. Since μmechanical circuits exhibit low-loss and consume virtually no dc power, such a device can greatly reduce the power consumption in transceivers, as will soon be seen.

2.6. Micromechanical Switches

The mixer-filter device described above is one example of a μmechanical circuit that harnesses nonlinear device properties to provide a useful function. Another very useful mode of operation that further utilizes the nonlinear nature of the device is the μmechanical switch. Figure 7 presents an operational schematic for a single-pole, single-throw μmechanical switch, seen to have a structure very similar to that of the previous resonator devices: a conductive beam or membrane suspended above an actuating electrode [16]. The operation of the switch of Fig. 7 is fairly simple: To achieve the "on-state", apply a sufficiently large volt-
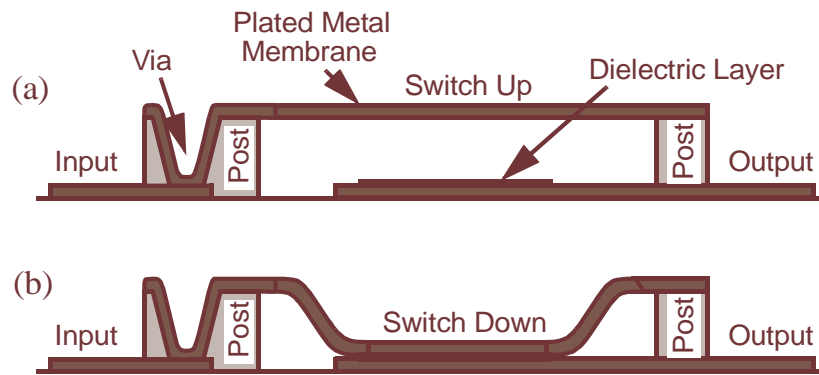
Figure 7: Cross-sectional schematics of a typical μmechanical switch: (a) Switch up. (b) Switch down [16].

age across the beam and electrode to pull the beam down and short it (in either a dc or ac fashion) to the electrode.

In general, to minimize insertion loss, the majority of switches use metals as their structural materials. It is their metal construction that makes μmechanical switches so attractive, allowing them to achieve "on-state" insertion losses down to 0.1 dB—much lower than FET transistor counterparts, which normally exhibit ~2 dB of insertion loss. In addition to exhibiting such low insertion loss, μmechanical switches are extremely linear, with *IIP3*'s greater than 66 dBm [1], and can be designed to consume no dc power (as opposed to FET switches, which sink a finite current when activated).

3. MEMS-Based Transceiver Architectures

Perhaps the most direct way to harness μmechanical circuits is via direct replacement of the off-chip ceramic, SAW, and crystal resonators used in RF preselect and image reject filters, IF channel-select filters, and crystal oscillator references in conventional super-heterodyne architectures. In addition, μmechanical switches can be used to replace FET T/R switches to greatly reduce wasted power in transmit mode (by as much as 280mW if the

desired output power is 500mW). Furthermore, medium-Q micromachined inductors and tunable capacitors [1], [17], [18] can be used in VCO's and matching networks for further miniaturization.

Although beneficial, the performance gains afforded by mere direct replacement by MEMS are quite limited when compared to more aggressive uses of MEMS technology. To fully harness the advantages of μmechanical circuits, one must first recognize that due to their micro-scale size and zero dc power consumption, μmechanical circuits offer the same system complexity advantages over off-chip discrete components that planar IC circuits offer over discrete transistor circuits. Thus, to maximize performance gains, μmechanical circuits should be utilized in large numbers.

Figure 8 presents the system-level block diagram for a possible transceiver front-end architecture that takes full advantage of the complexity achievable via μmechanical circuits. The main driving force behind this architecture is power reduction, attained in several of the blocks by replacing active components by low-loss passive μmechanical ones, and by trading power for high selectivity (i.e., high-Q). Among the key performance enhancing features are: (1) an RF channel selector comprised of a bank of switchable μmechanical filters, offering multi-band reconfigurability,
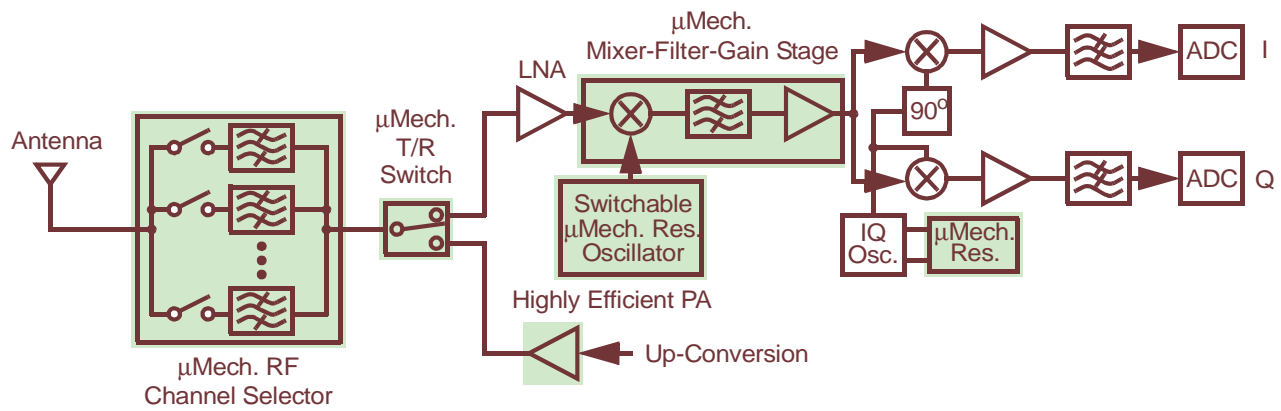
Figure 8: System block diagram for an RF channel-select receiver architecture utilizing large numbers of micromechanical resonators in banks to trade *Q* for power consumption. (On-chip μmechanics are shaded.)

receive power savings via relaxed dynamic range requirements [12], and transmit power savings by allowing the use of a more efficient power amplifier; (2) use of a passive μmechanical mixer-filter to replace the active mixer normally used, with obvious power savings; (3) a VCO referenced to a switchable bank of μmechanical resonators, capable of operating without the need for locking to a lower frequency reference, hence, with orders of magnitude lower power consumption than present-day synthesizers; (4) use of a μmechanical T/R switch, with already described power savings in transmit-mode; and (5) use of μmechanical resonator and switch components around the power amplifier to enhance its efficiency.

4. Circuits/MEMS Merging Technologies

Although a two-chip solution that combines a MEMS chip with a transistor chip can certainly be used to interface μmechanical circuits with transistor circuits, such an approach becomes less practical as the number of μmechanical components increases. For instance, practical implementations of the switchable filter bank in Fig. 8 require multiplexing support electronics that must interconnect with each

μmechanical device. If implemented using a two-chip approach, the number of chip-to-chip bonds required could become quite cumbersome, making a single-chip solution desirable.

In the pursuit of single-chip systems, several technologies that merge micromachining processes with those for integrated circuits have been developed and implemented over the past several years [2]-[7]. Figure 9 presents the cross-section and overhead SEM of one such technology that combined CMOS transistor circuits and polysilicon surface micromachined structures in a fully planar, modular fashion, where transistor and MEMS fabrication steps were separated into modules, and no intermixing of process steps from each process was permitted [4]. Such *modular* processes are advantageous, because they allow the greatest flexibility when changes are made to either the transistor or MEMS process steps.

In addition to fully planar integration methods, bonding processes, in which circuits and μmechanics are merged by bonding one onto the wafer of the other, are presently undergoing a resurgence [19]. In particular, the advent of more sophisticated aligner-bonder instruments are now making possible much smaller bond pad sizes, which soon may enable wafer-level bonding with bond pad sizes small
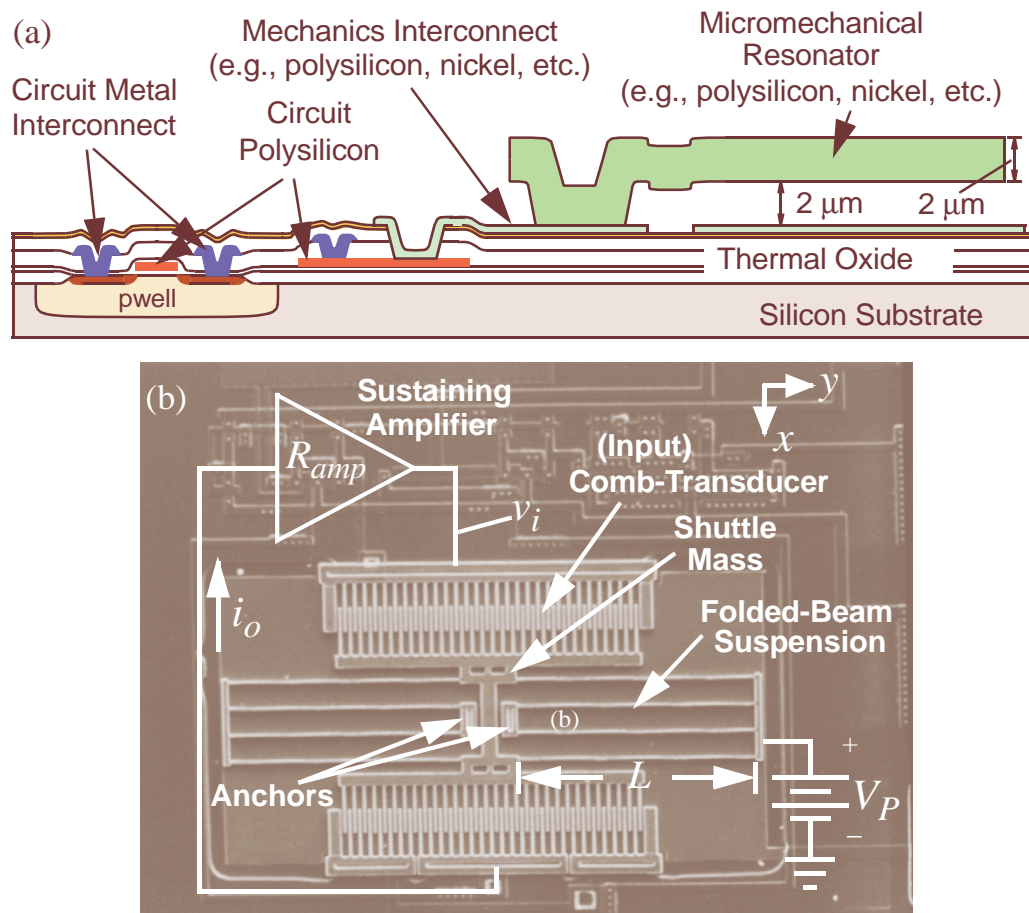
Figure 9: (a) Cross-section of the MICS process [4]. (b) Overhead-view of a fully integrated micromechanical resonator oscillator fabricated using MICS [8].

enough to compete with fully planar processed merging strategies in interface capacitance values. If the bond capacitance can indeed be lowered to this level with acceptable bonding yields, this technology may well be the ultimate in modularity.

From a broader perspective, the integration techniques discussed above are really methods for achieving low capacitance packaging of microelectromechanical systems. As mentioned in Section 2, another level of packaging is required to attain high Q vibrating μmechanical resonators: vacuum encapsulation. Although the requirement for vacuum is unique to vibrating μmechanical resonators, the requirement for encapsulation is nearly universal for all of the μmechanical devices discussed in this paper, and for virtually all micromechanical devices in general. In partic-

ular, some protection from the environment is necessary, if only to prevent contamination by particles (or even by molecules), or to isolate the device from electric fields or feedthrough currents. Needless to say, wafer-level encapsulation is presently the subject of intense research [20].

5. Conclusions

Micromechanical circuits attained via MEMS technologies have been described that can potentially play a key role in removing the board-level packaging requirements that currently constrain the size of communication transceivers. In addition, by combining the strengths of integrated μmechanical and transistor circuits, using both in massive quantities, previously unachievable functions become

possible that may soon enable alternative transceiver architectures with substantial performance gains, especially from a power perspective. However, before generating too much enthusiasm, it should be understood that RF MEMS technology is still in its infancy, and much research is needed (e.g., on frequency extension, trimming methods, vacuum encapsulation, and much more) before fully-integrated RF MEMS systems can become a reality.

References

[1] C. T.-C. Nguyen, L. P.B. Katehi, and G. M. Rebeiz, "Micromachined devices for wireless communications (invited)," *Proc. IEEE,* vol. 86, no. 8, pp. 1756-1768, Aug. 1998.

[2] T. A. Core, W. K. Tsang, S. J. Sherman, "Fabrication technology for an integrated surface-micromachined sensor," *Solid State Technology*, pp. 39-47, Oct. 1993.

[3] J. H. Smith, S. Montague, J. J. Sniegowski, J. R. Murray, *et al*., "Embedded micromechanical devices for the monolithic integration of MEMS with CMOS," *Proceedings*, IEEE IEDM, Washington, D.C., Dec. 10-13, 1995, pp. 609-612.

[4] J. M. Bustillo, G. K. Fedder, C. T.-C. Nguyen, and R. T. Howe, "Process technology for the modular integration of CMOS and polysilicon microstructures," *Microsystem Technologies*, **1** (1994), pp. 30-41.

[5] A. E. Franke, D. Bilic, D. T. Chang, P. T. Jones, T.-J. King, R. T. Howe, and G. C. Johnson, "Post-CMOS integration of germanium microstructures," *Technical Digest*, 12th Int. IEEE MEMS Conf., Orlando, FA, Jan. 17-21, 1999, pp. 630-637.

[6] H. Baltes, O. Paul, and O. Brand, "Micromachined thermally based CMOS microsensors," *Proc. IEEE*, vol. 86, no. 8, pp. 1660-1678, Aug. 1998.

[7] G. K. Fedder, S. Santhanam, M. L. Reed, S. C. Eagle, D. F. Guillou, M. S.-C. Lu, and L. R. Carley, "Laminated high-aspect-ratio microstructures in a conventional CMOS process," *Sensors and Actuators*, vol. A57, no. 2, pp. 103-110, March 1997.

[8] C. T.-C. Nguyen and R. T. Howe, "An integrated CMOS micromechanical resonator high-*Q* oscillator," *IEEE J. Solid-State Circuits*, vol. 34, no. 4, pp. 440-445, April 1999.

[9] F. D. Bannon III, J. R. Clark, and C. T.-C. Nguyen, "High frequency micromechanical filters," *IEEE J. Solid-State Circuits*, vol. 35, no. 4, pp. 512-526, April 2000.

[10] Q. Meng, M. Mehregany, and R. L. Mullen, "Theoretical modelling of micro-fabricated beams with elastically restrained supports," *J. Microelectromech. Syst*., vol. 2, no. 3, pp. 128-137, Sept. 1993.

[11] A. N. Cleland and M. L. Roukes, "Fabrication of high frequency nanometer scale mechanical resonators from bulk Si crystals," *Appl. Phys. Lett.*, **69** (18), pp. 2653-2655, Oct. 28, 1996.

[12] C. T.-C. Nguyen, "Frequency-selective MEMS for miniaturized low-power communication devices," *IEEE Trans. Microwave Theory Tech*., vol. 47, no. 8, pp. 1486-1503, Aug. 1999.

[13] K. Wang, Y. Yu, A.-C. Wong, and C. T.-C. Nguyen, "VHF free-free beam high-*Q* micromechanical resonators," *Technical Digest,* 12th Int. IEEE MEMS Conference, Orlando, Florida, Jan. 17-21, 1999, pp. 453-458.

[14] A.-C. Wong, J. R. Clark, and C. T.-C. Nguyen, "Anneal-activated, tunable, 68MHz micromechanical filters" *Digest of Technical Papers*, 10th Int. Conf. on Solid-State Sensors and Actuators, Sendai, Japan, June 7-10, 1999, pp. 1390-1393.

[15] A.-C. Wong, H. Ding, and C. T.-C. Nguyen, "Micromechanical mixer+filters," *Technical Digest,* IEEE IEDM, San Francisco, California, Dec. 6-9, 1998, pp. 471-474.

[16] C. Goldsmith, J. Randall, S. Eshelman, T. H. Lin, D. Denniston, S. Chen and B. Norvell, "Characteristics of micromachined switches at microwave frequencies," IEEE MTT-S Digest, pp. 1141-1144, June, 1996.

[17] D. J. Young and B. E. Boser, "A micromachined variable capacitor for monolithic low-noise VCOs," Technical Digest, 1996 Solid-State Sensor and Actuator Workshop, Hilton Head Island, South Carolina, June 3-6, 1996, pp. 86-89.

[18] J.-B. Yoon, C.-H. Han, E. Yoon, and C.-K. Kim, "Monolithic high-Q overhand inductors fabricated on silicon and glass substrates," *Technical Digest,* IEEE IEDM, Washington, D. C., Dec. 5-8, 1999, pp. 753-756.

[19] A. Singh, D. A. Horsley, M. B. Cohn, A. P. Pisano, and R. T. Howe, "Batch transfer of microstructures using flip-chip solder bonding," *J. Microelectromech. Syst.*, vol. 8, no. 1, pp. 27-33, March 1999.

[20] K. S. Lebouitz, A. Mazaheri, R. T. Howe, and A. P. Pisano, "Vacuum encapsulation of resonant devices using permeable polysilicon," *Technical Digest,* 12th Int. IEEE MEMS Conf., Orlando, Florida, Jan. 17-21, 1999, pp. 470-475.